
Parallelizing Linear Recurrent Neural Nets Over Sequence Length

Eric Martin
eric@ericmart.in

Chris Cundy
c.cundy@berkeley.edu

Abstract

Recurrent neural networks (RNNs) are widely used to model sequential data but their non-linear dependencies between sequence elements prevent parallelizing training over sequence length. We show the training of RNNs with only linear sequential dependencies can be parallelized over the sequence length using the parallel scan algorithm, leading to rapid training on long sequences with small minibatch size. We develop a parallel linear recurrence CUDA kernel and show that it can be applied to immediately speed up several RNN architectures by up to a factor of 9. We abstract recent work on linear RNNs into a new framework of linear surrogate RNNs and develop a linear surrogate for the long short-term memory unit, the GILR-LSTM, which is able to achieve throughput 30 times greater than the currently fastest-available LSTM implementation. We show that the GILR-LSTM is able to perform well on real-world problems,

Thought:
we could
rephrase this
as allowing
us to break
the necessity
of using large
batches to
train fast

1 Introduction

Recurrent neural networks (RNNs) are widely used for sequence modelling tasks in domains such as natural language processing [18], speech recognition [2], and reinforcement learning [10]. Most RNNs, including popular variants such as long short-term memories (LSTMs) [11] and gated recurrent units (GRUs) [6], contain a non-linear dependency between sequential inputs. These non-linear dependencies create a very flexible class of models but limit the feasibility of training RNNs on long sequences as each sequence element must be processed sequentially. Modelling sequences of thousands to millions of elements is important to domains such as robotics, remote sensing, control systems, speech recognition, medicine, and finance.

The RNN serial evaluation inefficiency problem is usually mitigated by parallelizing the forward and backward pass over a minibatch of inputs. Without minibatches, RNN evaluation is a sequence of matrix-vector multiplications. Minibatches transform RNN computation into a sequence of more efficient matrix-matrix multiplications, but this speed-up brings several disadvantages. RNN model size is often limited by GPU memory size, and running a forward and backward pass on a minibatch requires memory linear in the minibatch size. Grouping data into minibatches increases the latency of each pass and reduces the rate of optimization steps. Finally, training with larger minibatches damages generalization ability [13]. It is clearly important to investigate if it is possible to parallelise RNN training without introducing minibatches. Persistent RNNs [7] use a novel implementation that can achieve high GPU utilization with very small minibatch sizes when the recurrent state is larger than 500 elements, but even persistent RNNs become limited by the serial evaluation inefficiency at smaller hidden sizes.

Numerous prior works have shown strong performance from neural sequential models with only linear dependence on earlier sequence elements. Balduzzi and Ghifary [3] investigated RNNs with only elementwise linear recurrence relations $h_t = \alpha_t \odot h_{t-1} + (1 - \alpha_t) \odot x_t$ and developed linear variants of LSTM and GRU that perform similarly to standard non-linear RNNs on text generation tasks. Bradbury et al. [5], Kalchbrenner et al. [12], Gehring et al. [8], and van den Oord et al. [19] have successfully applied networks of convolutions over sequences for tasks such as machine translation,

language modelling, and audio generation. These works have observed up to an order of magnitude increase in training throughput compared to RNN alternatives. Convolutional sequence models typically rely on either an attention mechanism or a (possibly linear) recurrent layer to integrate information at scales larger than the filter width. Introduction of a recurrent layer prevents full parallelization over the sequence length while attention mechanisms are expensive to apply on long sequences in online inference use cases. One dimensional convolution can be viewed as a learnable linear finite impulse response (FIR) filter with a parallel evaluation algorithm, while linear recurrence is a learnable linear infinite impulse response (IIR).

Seems like an aside - take out?

This work parallelizes evaluation of linear recurrences through application of the parallel scan algorithm.

Scans and reductions are computations involving repeated application of a binary operator \oplus over an array of data. Computing the sum or maximum of an array is an example of a reduction, while a cumulative sum is a common example of a scan operation. Throughout this work, the scan of \oplus with initial value b is defined as

$$\text{SCAN}(\oplus, [a_1, a_2, \dots, a_n], b) = [(a_1 \oplus b), (a_2 \oplus a_1 \oplus b), \dots, (a_n \oplus a_{n-1} \dots \oplus a_1 \oplus b)]$$

The reduction of \oplus over array A and initial value b is denoted $\text{REDUCE}(\oplus, A, b)$ and is the final element of $\text{SCAN}(\oplus, A, b)$. Despite their dependent computation graph, algorithms exist to parallelize scans and reductions when \oplus is associative [15].

Blelloch [4] shows that first order recurrences of the form $h_t = (\Lambda_t \otimes h_{t-1}) \oplus x_t$ can be parallelized with the parallel scan algorithm if three conditions are met:

1. \oplus is associative: $(a \oplus b) \oplus c = a \oplus (b \oplus c)$
2. \otimes is semiassociative: there exists a binary associative operator \odot such that $a \otimes (b \otimes c) = (a \odot b) \otimes c$
3. \otimes distributes over \oplus : $a \otimes (b \oplus c) = (a \otimes b) \oplus (a \otimes c)$

Considering the familiar operations in linear algebra, we see that the associative operation of vector addition ($\mathbf{x} \oplus \mathbf{y} = \mathbf{x} + \mathbf{y}$), the semiassociative operation of matrix-vector multiplication ($A \otimes \mathbf{x} = A\mathbf{x}$) and the associative operation of matrix-matrix multiplication ($A \odot B = AB$) satisfy Blelloch's three conditions, allowing $h_t = \Lambda_t h_{t-1} + x_t$ to be evaluated in parallel over time steps t for vectors x_t and square matrices Λ_t .

We investigate this idea further and deliver the following contributions:

- We classify the RNNs which satisfy the conditions above, and show that many of the RNNs used in practice such as the Quasi-RNN are contained in this class
- We provide an implementation of the parallel linear recurrence algorithm as a CUDA kernel, and show that it speeds up training of the SRU and QRNN architectures by factors of up to 9x
- We describe how several recent linear RNNs can be described as linear surrogates for nonlinear architectures. We introduce a linear surrogate for the LSTM and show that we are able to train it with a speedup of 5-10x compared to the CuDNN-LSTM when we use the parallel linear recurrence algorithm.

2 Parallel linear recurrence

As the method is essential to this work, Algorithm 1 presents the parallel linear recurrence algorithm for the interested reader.

2.1 Theoretical performance

The cost of a serial scan over a sequence of length T is $C_{\text{sscan}} \in \mathcal{O}((C_{\otimes} + C_{\oplus})T)$, compared to the parallel scan cost $C_{\text{pscan}} \in \mathcal{O}(2(C_{\odot} + C_{\otimes} + C_{\oplus})(T/p + \lg p))$ [4], where p is the number of available parallel cores. If h_t is a vector of dimension n then $C_{\odot} \in \mathcal{O}(n^3)$, $C_{\otimes} \in \mathcal{O}(n^2)$, $C_{\oplus} \in \mathcal{O}(n)$ giving $C_{\text{pscan}} \in \mathcal{O}(2(n^3 + n^2 + n)(T/p + \lg p))$ and $C_{\text{sscan}} \in \mathcal{O}((n^2 + n)T)$. The $\mathcal{O}(n^3)$ cost of the matrix

Algorithm 1 Parallel linear recurrence on p processors

```
1: Let  $y = [(\Lambda_1, x_1), (\Lambda_2, x_2), \dots, (\Lambda_T, x_T)]$ 
2: Let binary operator  $\bullet$  act as  $(\Lambda, x) \bullet h = \Lambda h + x$ 
3: Let  $S_0 = 1, S_i < E_i, E_i + 1 = S_{i+1}, E_{p-1} = T$  for  $i$  in  $0, p-1$ 
4:
5: parfor  $i \leftarrow 0, p-1$  do
6:    $P_i = \text{REDUCE}(\odot, \Lambda_{S_i:E_i}, I)$ 
7:    $R_i = \text{REDUCE}(\bullet, y_{S_i:E_i}, 0)$ 
8: end parfor
9:
10: Let  $z = [(P_0, R_0), (P_1, R_1), \dots, (P_p, R_p)]$ .
11:  $C = \text{SCAN}(\bullet, z, h_0)$   $\triangleright$  compute  $C_i = P_i C_{i-1} + R_i$  with  $C_{-1} = h_0$ 
12:
13: parfor  $i \leftarrow 0, p-1$  do
14:    $h_{S_i:E_i} = \text{SCAN}(\bullet, y_{S_i:E_i}, C_{i-1})$ 
15: end parfor
16: return  $h$ 
```

multiplication in the parallel algorithm can counter-act any parallel speedups for sufficiently large hidden states and lead to a slower algorithm overall.

To avoid this problem, we will only consider diagonal matrices Λ_t , in which case both matrix-matrix and matrix-vector multiplication have cost proportional to n and $C_{\text{pscan}} \in \mathcal{O}(6n(T/p + \lg p))$ and $C_{\text{sscan}} \in \mathcal{O}(2nT)$. Assuming $p \ll T$, then $C_{\text{pscan}} \leq C_{\text{sscan}}$ when $p \geq 3$. As we are only considering diagonal matrices, we write the linear recurrence as $h_t = \lambda_t \odot h_{t-1} + x_t$ where \odot indicates elementwise multiplication.

Limiting Λ_t to be diagonal may seem like a severe constraint but there are several reasons to do so beyond the unfavorable parallelization performance. Relatively few neural network models use separate recurrent matrices for each sequence element and using these separate matrices would require potentially prohibitive $n^2 T$ memory. Applying the same matrix Λ to each sequence element is also unappealing considering that a matrix multiplication can be thought of as a rotation and a scaling. The same rotation at every element seems unlikely to be useful, and the scaling is exactly what's captured in diagonal vectors λ_t . Recurrent coefficient vectors λ_t provide enough flexibility to implement schemes such as exponential moving averages or a gating mechanism.

Can include the actual speedup factor, $\alpha = \frac{PT}{3(T+\lg(p))}$.

I can't seem to find anyone explicitly saying this before from a quick google.

2.2 Backpropagation

$$\begin{aligned}\nabla_{h_T} L &= \frac{\partial L}{\partial h_T} \\ \nabla_{h_t} L &= \frac{\partial h_{t+1}}{\partial h_t} \odot \nabla_{h_{t+1}} L + \frac{\partial L}{\partial h_t} \\ &= \lambda_{t+1} \odot \nabla_{h_{t+1}} L + \frac{\partial L}{\partial h_t} \\ \nabla_{\lambda_t} L &= \frac{\partial h_t}{\partial \lambda_t} \odot \nabla_{h_t} L = h_{t-1} \odot \nabla_{h_t} L \\ \nabla_{x_t} L &= \nabla_{h_t} L \\ \nabla_{h_0} L &= \frac{\partial h_1}{\partial h_0} \odot \nabla_{h_1} L = \lambda_1 \odot \nabla_{h_1} L\end{aligned}$$

The backpropagation equations center around a linear recurrence over $\frac{\partial L}{\partial h_t}$ in the reverse order of the original sequence. This allows for parallelizing both the forwards and backwards pass of a linear RNN over the sequence length.

2.3 Implementation

In 2017, GPUs commonly used in deep learning consist of between 640 and 3200 concurrently executing warps. Each warp operates on 32 single precision floating point numbers in parallel.

This work implemented parallel linear recurrence as a CUDA kernel with bindings into the TensorFlow [1] framework. Each warp acts as a processor, which means the algorithmic parallelizability p is up to 3200 and the theoretical parallelization speedup factor is up to several hundred. The 32 lanes of each warp work on different elements of the recurrence vector in parallel. These implementation details mean that peak performance is only obtained on sequences of at least several thousand steps on at least a 32 element vector.

3 Models

Parallel linear recurrence can be used to construct a wide variety of differentiable modules that can be evaluated in parallel. Common applications of linear recurrence include gating schemes and exponential moving averages. Although linear recurrence values can depend only linearly on previous elements, the stacking of linear recurrent layers separated by non-linearities allows for a non-linear dependence on the past. In this sense the non-linear depth of a linear recurrent network is the number of layers and not the sequence length.

3.1 Gated impulse linear recurrent layer

A gated impulse linear recurrent (GILR) layer transforms its m dimensional inputs x_t into a sequence of n dimensional hidden states h_t :

$$\begin{aligned}g_t &= \sigma(Ux_t + b_g) \\i_t &= \tau(Vx_t + b_z) \\h_t &= g_t \odot h_{t-1} + (1 - g_t) \odot i_t\end{aligned}$$

A GILR layer applies the same non-linear transform to each sequence element and then accumulates the sequence elements with a non-linear gating mechanism. Gate g_t uses the sigmoid activation function to give values in $[0,1]$ for reasonable gating semantics, while impulse i_t can use any activation function τ . Stacking GILR layers allows for rich non-linear dependence on previous events while still taking advantage of fast parallel sequence evaluation.

3.1.1 Impact on effective "batch size"

Consider evaluating an RNN with recurrence $h_t = \sigma(Uh_{t-1} + Vx_t + b)$, from m inputs to n hidden units on a sequence of length T with minibatch size b using a serial evaluation strategy. At each of T iterations, the naive approach performs two $(b, m) \times (m, n)$ matrix multiplications. Larger matrix multiplications achieve higher throughput due to less IO overhead, so the better approach computes Vx_t for all t ahead of time in a single $(bT, m) \times (m, n)$ matrix multiply. The non-linear recurrence forces even the better approach to perform T potentially small $(b, m) \times (m, n)$ matrix multiplications in serial which makes performance heavily dependent on minibatch size.

Now consider the GILR, noting that it has the same two matrix-vector multiplications per iteration as the above RNN. The intermediate variables g and i can be evaluated for all t with a single $(bT, m) \times (m, n)$ matrix multiplication each. Given g and i , h can be computed using a parallel linear recurrence over T vectors each of bn elements. Rather than T small operations, the GILR can be evaluated over all sequence elements with two large matrix multiplications and a parallel linear recurrence. GILR performance is much less dependent on batch size as the matrix multiplies see an "effective batch size" of bT and T is typically large.

3.2 Linear surrogate RNNs

RNNs learn a transition function $s_t = f(s_{t-1}, x_t)$ which combines previous state s_{t-1} with input x_t to compute current state s_t . Non-linear f prevents application of the parallel linear recurrence algorithm and forces slow serial evaluation. To work around this inefficiency, note that s_t serves a dual purpose. In $s_t = f(s_{t-1}, x_t)$, s_{t-1} serves as an input to f summarizing the previous inputs while

s_t serves as the output of f to be passed to other layers of the network. We can decouple these uses and introduce independent variables for each purpose: s_t is passed onto other layers of the network and we introduce the linear surrogate \tilde{s}_t which is passed onto the next state, with $s_t = f(\tilde{s}_{t-1}, x_t)$. We are still able to choose a nonlinear f , our only limitation being that \tilde{s}_t must be linearly computable. We refer to this class of model as a linear surrogate RNN (LS-RNN). Quasi-RNNs [5] are LS-RNNs using $\tilde{h}_{t-1} = W_k x_{t-k} + \dots W_1 x_{t-1}$ and strongly typed RNNs[3] are LS-RNNs with $\tilde{h}_t = x_{t-1}$. Although not a rule, LS-RNNs can often be parallelized over sequence length with either convolution or linear recurrence.

As an example LS-RNN, consider an LSTM:

$$\begin{aligned} f_t, i_t, o_t &= \sigma(U_{f,i,o} h_{t-1} + V_{f,i,o} x_t + b_{f,i,o}) \\ z_t &= \tau(U_z h_{t-1} + V_z x_t + b_z) \\ c_t &= f_t \odot c_{t-1} + i_t \odot z_t \\ h_t &= o_t \odot c_t \end{aligned}$$

An LSTM has state $s_t = (h_t, c_t)$. Since c_t depends only linearly on c_{t-1} , no surrogate is needed for c_t . h_t has a non-linear dependence on h_{t-1} , so h_t needs a linear surrogate. Introducing a GILR layer as the surrogate, we obtain the GILR-LSTM:

$$\begin{aligned} f_t, i_t, o_t &= \sigma(U_{f,i,o} \tilde{h}_{t-1} + V_{f,i,o} x_t + b_{f,i,o}) \\ z_t &= \tau(U_z \tilde{h}_{t-1} + V_z x_t + b_z) \\ c_t &= f_t \odot c_{t-1} + i_t \odot z_t \\ h_t &= o_t \odot c_t \\ g_t &= \sigma(V_g x_t + b_g) \\ \tilde{h}_t &= g_t \odot \tilde{h}_{t-1} + (1 - g_t) \odot \tau(W x_t + b_h) \end{aligned}$$

For m inputs and hidden size n , the GILR-LSTM contains $2n(n + m)$ more parameters than the equivalently sized LSTM to handle the mapping from x to \tilde{h} . More generally, a LS-RNN contains all of the same parameters as the underlying RNN as well as some additional parameters to compute the linear surrogate.

4 Experiments

We perform several experiments, first confirming that our implementation of the parallel linear recurrence algorithm is able to achieve higher throughput than a similarly implemented serial version of the algorithm. We show that the plr kernel is up to 40 times faster than the serial equivalent for long sequence lengths, and that this speedup translates to implementations of LS-RNNs such as the QRNN (where we can get a speedup of up to 9 times).

In order to illustrate that the linearisation does not necessarily come at the cost of expressibility, we show that the GILR-LSTM architecture, trained with the PLR algorithm, is able to outperform the optimized CuDNN LSTM implementation on a pathological example from the original LSTM paper [11]. Finally we show that our GILR-LSTM is able to quickly achieve state of the art results on an existing medical data set.

I hope so...

4.1 Throughput Benchmarks

We first illustrate the throughput advantage of the parallel scan algorithm for evaluating the linear recurrence. For a minibatch comprised of b sequences of length T , we define the number of events as bT and the throughput as the number of events per second. We implement two CUDA kernels, one which evaluates the parallel linear recurrence described in algorithm 2, and one which evaluates the linear recurrence using the straightforward serial approach. This comparison is performed directly at the kernel level, avoiding any overhead due to calling Tensorflow. We find that at long sequence lengths, the PLR kernel has a distinct advantage, as shown in table 1, with a speedup factor of 40. At short sequence lengths, the parallel kernel does not perform well due to the extra overhead involved in marshalling the parallel algorithm.

Important: What's the batch size here? Is it just one sequence? Need to say that

Table 1: Speedup of the PLR kernel compared to the SLR kernel, without any overhead from Tensorflow, for various sequence lengths and input size m .

Sequence Length	$m = 4$	$m = 32$	$m = 128$
16	0.06	0.06	0.05
256	0.22	0.22	0.86
4,096	1.02	2.94	3.36
65,536	38.5	41.8	17.5

Sequence Length	GILR-LSTM	SRU	QRNN(2)	QRNN(10)
16	0.61	0.28	0.38	0.78
256	0.91	0.84	0.86	0.99
4,096	0.98	1.38	1.18	1.05
65,536	1.41	9.21	6.68	2.05

Figure 1: Speedup obtained when using parallel linear recurrence compared to serial linear recurrence. We analyse this for several recent architectures: the Simple Recurrent Unit from [20], the Quasi-RNN from [5], with a convolutional filter of size 2 and 10, and the GILR-LSTM which we introduce in section 3.2. To give a fair model of a typical use-case maximising the memory usage of the GPU, we set batch size b such that $Tb = 65536$ for a sequence length T .

Many of the RNNs that have been recently introduced can be implemented with a parallel linear recurrence. Table 4.1 shows the throughput advantage by using a parallel linear recurrence when compared to a serial linear recurrence. Since PLR and SLR are simply different methods for computing the recurrence, there is no penalty incurred for this speedup - we obtain exactly the same output.

Typically experiments will aim to maximize the memory utilisation of the GPU, so we simulate this by choosing the product of the batch size and the sequence length to be constant. We see that the architectures which have fewer terms (for which the linear recurrence is a higher proportion of the computational burden) are more effected by the switch to PLR. This is particularly clear in the case of the QRNN, where including a wider convolutional window results in less time spent on the recurrence and less to gain from the parallelization.

Finally, we compare the throughput of the linear surrogate LSTM to the current fastest available implementation of the LSTM, the CuDNN-LSTM. Figure 2 shows that our GILR-LSTM has higher throughput for most of the low-batch-size regime, with a 30x speedup at a sequence length of 65,536. Recent work [13] has suggested that small mini-batches may aid generalization by encouraging the discovery of shallow minima. The GILR-LSTM allows us to achieve high throughput for all choices of minibatch size and sequence length.

Unlike the previous case, these speedups do come at a cost. The GILR-LSTM architecture is different to the canonical LSTM, and it’s possible that the loss of model capacity outweighs the speedup in training. The following experiment shows that the GILR-LSTM is able to outperform the LSTM on an example originally designed to illustrate the advantages of the LSTM.

4.2 Synthetic Example

In order to demonstrate how PLR may be used to speed up tasks that the LSTM is well-suited for, we tackle a pathological inference problem. Originally introduced as example 2b from Hochreiter and Schmidhuber’s introduction of the LSTM, [11], it involves storing a number for a very long sequence of time steps. We have an alphabet of size p with each character represented as a particular one-hot vector in this space. We input a sequence of n of these vectors, chosen at random (with replacement). The first vector in the sequence is always the same, up to the sign of the component (i.e. it is $\pm p_0$).

The two signs on the first component separate the sequences into two sets. The whole sequence is fed into the LSTM and we aim to learn to classify the sequences. This requires remembering the first element over the length of the sequence. Due to the large throughput of the GILR-LSTM, we would expect that it would do better when the sequence length is large. In the original formulation of the

batch size	LSTM									
	1	2	4	8	16	32	64	128	256	
	14.3	18.4	37.1	90.8	170	305	534	695	772	
seq length	LS-LSTM									
	256	63.6	124	226	323	390	448	467	467	464
	512	118	227	304	388	460	477	474	474	471
	1024	189	304	375	435	475	467	463	459	
	2048	311	405	469	491	502	497	491		
	4096	412	471	503	509	517	509			
	8192	478	509	514	521	520				
	16384	510	512	520	527					
	32768	510	510	517						
	65536	509	511							
	131072	503								

Table 2: Throughput comparison between LSTM-256-256 with GILR-LSTM-256-256, with a 32-dimensional input and a 2-dimensional output, for various batch sizes and sequence lengths. The LSTM only has a single row of data because its throughput is independent of sequence length. Entries are missing from the GILR-LSTM table because there was not enough memory on the GPU to handle such large batch sizes and sequences.

problem (dealing in the regime with around one hundred timesteps), p is set equal to n . Since this would make the size of the input data grow impractically large as $\mathcal{O}(n^2)$ for long sequences, we fix $p = 128$ and vary n .

We generated three sets of data: for n equal to 1,024, 8,192, and 1,048,576. For each of these we compared a two-layer GILR-LSTM with 512 hidden units to a canonical LSTM network with roughly the same number of parameters. We could imagine using a two-layer LSTM with 512 hidden units in each layer, or a one-layer LSTM with 1024 hidden units.

Initial experiments showed that the two-layer LSTM was much quicker to converge than the one-layer LSTM, so here we compare the GILR-LSTM to the two-layer CudnnLSTM. We ran all experiments on a NVIDIA K80 GPU, choosing the largest minibatch size which fit into the GPU memory, with five runs per configuration allowing us to find the average and standard deviation of the time and number of iterations to convergence. For all CUDA runs, a brief search over learning rate and batch size was carried out to find the parameters which allow the network to converge most rapidly. The criterion for convergence was five consecutive minibatches giving 100% accuracy. As can be seen from the learning curves in figure 2, this was a reasonable criterion. For the longest sequence-length, we didn't observe the CuDNN-LSTM converging.

The results illustrate that the GILR-LSTM is able to robustly outperform the CuDNN-LSTM, which is currently the fastest LSTM implementation available. This is somewhat surprising, as we might expect that the LSTM would do particularly well at an example that was specifically constructed for it. We can conclude that the nonlinearities in the LSTM's design are not vital for its performance given that the linear GILR-LSTM is able to converge, and that if these nonlinearities are not completely necessary, they entail a large performance cost by diallowing the plr algorithm from being used.

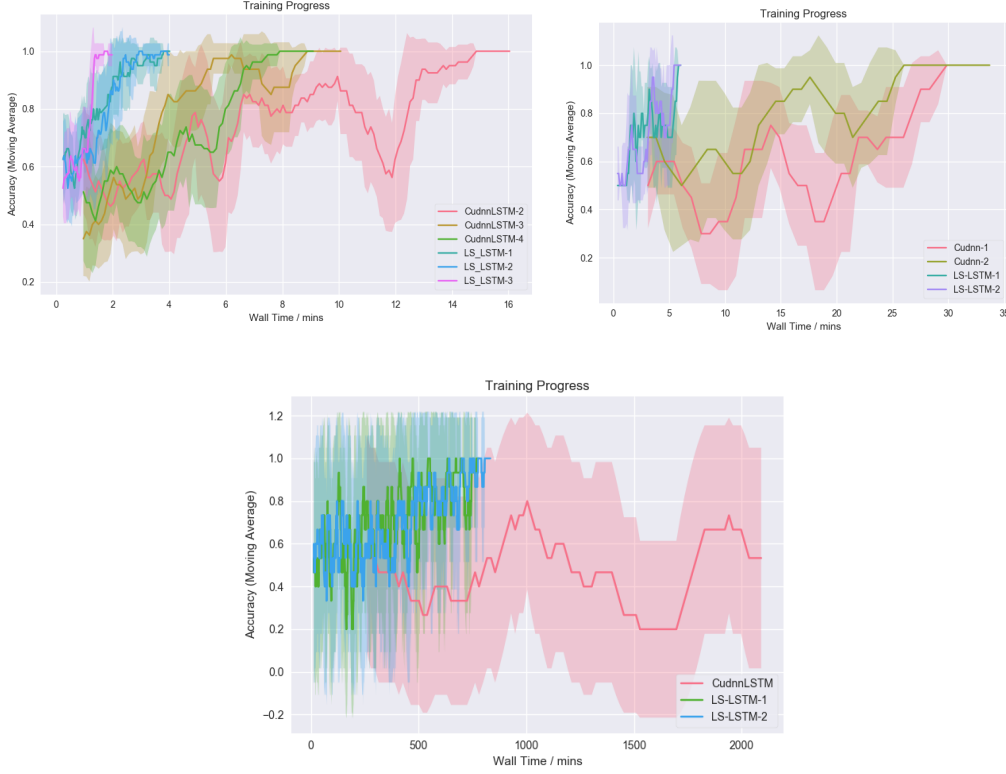


Figure 2: Training curves for GILR-LSTM and CUDNNLSTM architectures for various sequence lengths. (Clockwise from top-left: 1024, 8192, 1048576)

Table 3: Performance of the GILR-LSTM compared to CUDA-optimised CudnnLSTM implementation on problem 2b from (cite '97). We see that the GILR-LSTM has a clear advantage in training speed as the sequence length increases. We did not observe the Cudnn-LSTM converging for the longest task, even after several days. *For the longest sequence length, the number of hidden units was decreased to 64 for both architectures so that the net could fit in memory.

Sequence Length	1,024		8,192		1,048,576*	
	CuDNN	G	C	GILR	CuDNN	GILR
Iterations (1000s)	1.0 ± 0.4	0.55 ± 0.04	0.44 ± 0.05	0.56 ± 0.16	-	14 ± 3
Wall Clock time (hours)	0.28 ± 0.08	0.031 ± 0.002	0.58 ± 0.06	0.10 ± 0.03	-	9.7 ± 1.7

4.3 The Medical Setting

A common application of RNNs is in medicine. In order to illustrate the increased performance that the plr algorithm allows, we implement an GILR-LSTM on the problem presented in , the 2016 PhysioNet/Computing in Cardiology Challenge 2016. The aim of the Classification of Normal/Abnormal Heart Sound Recordings challenge is to determine which of a set of EEGs are produced by people with abnormal hearts. The data is recorded from a variety of sources and split into a training and testing set. The testing set is not publicly available, but can be evaluated through a web portal. The top results cover a large range of techniques, but generally rely on featurization of the raw EEG records. We want to see if we are able to leverage our advantage at high sequence-lengths to train directly on the raw EEG. The EEGs are sampled at 2,000 Hz and range in length from several seconds to more than one hundred seconds, giving a max sequence length of over 200,000. Since the testing server is not equipped with a GPU, we cannot run PLR in the testing step. We resample the records to 250 Hz so that we are able to evaluate the test results in a reasonable amount of time, padding all records that are shorter than the longest.

CITE

The training set of data is unbalanced, with 75% of the data corresponding to normal hearts. We rebalance the data by oversampling the abnormal data by a factor of three, including each abnormal heart three times.

Key points are:

- With the fast training of the GILR-LSTM / PLR, we can train quickly on very long sequence-lengths
- Allows us to get state-of-the-art results, even when performing very quickly and with little hyperparameter tuning

NEED TO GET THOSE RESULTS!

Quite likely that the results won't be available for tomorrow, or that they won't be particularly impressive. We may have to scratch this entire section unfortunately

5 Conclusion

Parallel linear recurrence is an extremely powerful algorithm and the GILR-LSTM is just one of many possible models that can be built with it. While we were previously forced to use large minibatches in order to obtain reasonable training speed, with PLR in many cases we can train rapidly on small minibatch sizes, freeing us to utilise extremely long sequence lengths and more complex models. Our CUDA kernel is up to 40 times faster than a serial kernel on sequence lengths of 65,536, and this benefit transfers to implemented models, speeding up the SRU [20] by a factor of 9. The impressive results in [20] and other recent work comprehensively show that linearly-recurrent RNNs are, in many respects, equally as powerful as nonlinear LSTMs. Our results on the synthetic example continue this trend, showing that the GILR-LSTM is able to handle sequence length regimes that are longer than any we have seen seriously suggested in the literature. We feel that the framework of describing linear RNNs as linear surrogates for nonlinear RNNs is a fruitful approach, and that this, paired with the PLR algorithm, will substantially advance the ability to train RNNs, and to understand timeseries data.

We intend to expand upon the experiments section and open-source the parallel linear recurrence kernel in the near future.

Acknowledgments

We would like to acknowledge Kevin Bowers, Alex Meiburg, JD Co-Reyes, Carson McNeil, Andy Palan, and several others for fruitful conversations and guidance.

References

- [1] M. Abadi, A. Agarwal, P. Barham, E. Brevdo, Z. Chen, C. Citro, G. S. Corrado, A. Davis, J. Dean, M. Devin, et al. Tensorflow: Large-scale machine learning on heterogeneous distributed systems. *arXiv preprint arXiv:1603.04467*, 2016.

- [2] D. Amodei, R. Anubhai, E. Battenberg, C. Case, J. Casper, B. Catanzaro, J. Chen, M. Chrzanowski, A. Coates, G. Diamos, et al. Deep speech 2: End-to-end speech recognition in english and mandarin. *arXiv preprint arXiv:1512.02595*, 2015.
- [3] D. Balduzzi and M. Ghifary. Strongly-typed recurrent neural networks. In *Proceedings of The 33rd International Conference on Machine Learning*, pages 1292–1300, 2016.
- [4] G. E. Blelloch. Prefix sums and their applications. 1990.
- [5] J. Bradbury, S. Merity, C. Xiong, and R. Socher. Quasi-recurrent neural networks. In *International Conference on Learning Representations (ICLR)*, 2017.
- [6] K. Cho, B. Van Merriënboer, C. Gulcehre, D. Bahdanau, F. Bougares, H. Schwenk, and Y. Bengio. Learning phrase representations using rnn encoder-decoder for statistical machine translation. *arXiv preprint arXiv:1406.1078*, 2014.
- [7] G. Diamos, S. Sengupta, B. Catanzaro, M. Chrzanowski, A. Coates, E. Elsen, J. Engel, A. Hannun, and S. Satheesh. Persistent rnns: Stashing recurrent weights on-chip. In *International Conference on Machine Learning*, pages 2024–2033, 2016.
- [8] J. Gehring, M. Auli, D. Grangier, D. Yarats, and Y. N. Dauphin. Convolutional sequence to sequence learning. *arXiv preprint arXiv:1705.03122*, 2017.
- [9] X. Glorot and Y. Bengio. Understanding the difficulty of training deep feedforward neural networks. In *Aistats*, volume 9, pages 249–256, 2010.
- [10] M. Hausknecht and P. Stone. Deep recurrent q-learning for partially observable mdps. In *2015 AAAI Fall Symposium Series*, 2015.
- [11] S. Hochreiter and J. Schmidhuber. Long short-term memory. *Neural computation*, 9(8): 1735–1780, 1997.
- [12] N. Kalchbrenner, L. Espeholt, K. Simonyan, A. v. d. Oord, A. Graves, and K. Kavukcuoglu. Neural machine translation in linear time. *arXiv preprint arXiv:1610.10099*, 2016.
- [13] N. S. Keskar, D. Mudigere, J. Nocedal, M. Smelyanskiy, and P. T. P. Tang. On large-batch training for deep learning: Generalization gap and sharp minima. 2017.
- [14] D. Kingma and J. Ba. Adam: A method for stochastic optimization. *arXiv preprint arXiv:1412.6980*, 2014.
- [15] R. E. Ladner and M. J. Fischer. Parallel prefix computation. *Journal of the ACM (JACM)*, 27(4): 831–838, 1980.
- [16] Y. LeCun, C. Cortes, and C. J. Burges. The mnist database of handwritten digits, 1998.
- [17] G. Orchard, A. Jayawant, G. Cohen, and N. Thakor. Converting static image datasets to spiking neuromorphic datasets using saccades. *arXiv preprint arXiv:1507.07629*, 2015.
- [18] I. Sutskever, O. Vinyals, and Q. V. Le. Sequence to sequence learning with neural networks. In *Advances in neural information processing systems*, pages 3104–3112, 2014.
- [19] A. van den Oord, S. Dieleman, H. Zen, K. Simonyan, O. Vinyals, A. Graves, N. Kalchbrenner, A. Senior, and K. Kavukcuoglu. Wavenet: A generative model for raw audio. *CoRR abs/1609.03499*, 2016.
- [20] T. Lei, Y. Zhang, Training RNNs as fast as CNNs. *arXiv preprint arXiv:1709.02755*, 2017.